

SEISMIC PERFORMANCE NORMALIZATION OF BRIDGES USING A DAMPING-ENHANCED STRENGTHENING METHODOLOGY

G.D. Chen¹ and K. R. Karim²

¹ Professor, Dept. of Civil, Architectural, and Environmental Engineering, Missouri University of Science and Technology, Missouri, USA, Email: gchen@mst.edu

² Ph.D. Candidate, Dept. of Civil, Architectural, and Environmental Engineering, Missouri University of Science and Technology, Missouri, USA, Email: krk2q4@mst.edu

ABSTRACT:

In this paper, a viscoelastic layer is integrated into a fiber reinforced polymer strengthening jacket for the seismic retrofit of a three-span steel-girder bridge. The distributed damping layer is represented by a series of discrete and complex springs in the finite element model of bridge columns. Damping ensures that the bridge is operational under moderate earthquakes and strengthening mainly ensures the bridge safety under strong earthquakes. Together, they meet the multiple performance objectives under earthquakes of varying intensities.

KEYWORDS: Viscoelastic damping, fiber reinforced polymer jacketing, performance-based design

1. INTRODUCTION

Strengthening techniques such as fiber reinforced polymer (FRP) jacketing have been developed over the past two decades (FHWA, 1995; MCEER, 2005). These jacketing techniques can be used to effectively confine an existing reinforced concrete (RC) column to prevent it from collapsing during a strong earthquake. Strengthening alone, however, is unlikely to improve the column performance under moderate earthquakes since small column deformation does not allow the jacketing system fully engaged. Therefore, a damping-enhanced strengthening (DES) methodology was recently proposed by the first author to meet multiple performance objectives in performance-based design and retrofit of bridges (Chen *et al.*, 2006). The damping component is to reduce the column response under moderate earthquakes so that the operational performance objective of bridges can be met, while the strengthening component is effective for the safety performance objective.

This study is aimed at developing a spring representation of the damping component in the finite element model (FEM) of bridges, applying it to the analysis of a single bent of a three-span continuous steel girder bridge, and conceptualizing a retrofiting process and design of the bridge by evaluating the normalized performance of the DES methodology against multiple performance objectives.

2. DISCRETE AND COMPLEX SPRING MODELING OF A DAMPING LAYER

In the proposed methodology (Chen *et al.*, 2006), a viscoelastic layer is sandwiched between an inner and an outer FRP sheet. The inner FRP sheet provides confinement on the columns of a bridge. The outer FRP sheet is anchored into footing/capbeam of the columns, providing an amplified constraint effect on the shear deformation in a viscoelastic layer.

2.1. Shear Strain Amplification in VE Layer

To understand the effectiveness of a new constrained layer treatment in the DES methodology, consider a cantilevered column partially covered by a viscoelastic layer and subjected to a bending moment at the cantilever end. Figures 1 and 2 present a comparison of the shear stress distributions between the conventional and the new treatments. Under the end moment M_0 , the column experiences a constant moment or curvature along its height. When the constrained layer is not anchored as shown in Figure 1, the induced shear stress must be zero and change its direction at the middle height of the VE layer, and proportional to the distance from the middle height of the VE layer at other points to ensure the resultant of the distributed forces on the VE layer is zero.

On the other hand, when the constrained layer is anchored into the column footing as illustrated in Figure 2, the shear stress induced linearly increases with the distance from the footing in the same direction. As a result, the maximum stress in the new treatment, solid plus dotted arrows in Figure 2, is more than twice that of the conventional way as shown in Figure 1 (Kerwin and Ungar, 1990). By superimposing the stress distribution in Figure 1 with that in Figure 2, the net stress difference gained with the anchored constrained layer is indicated by the solid arrows in Figure 2, resulting in four times the shear force counteracting the effect of the end moment.

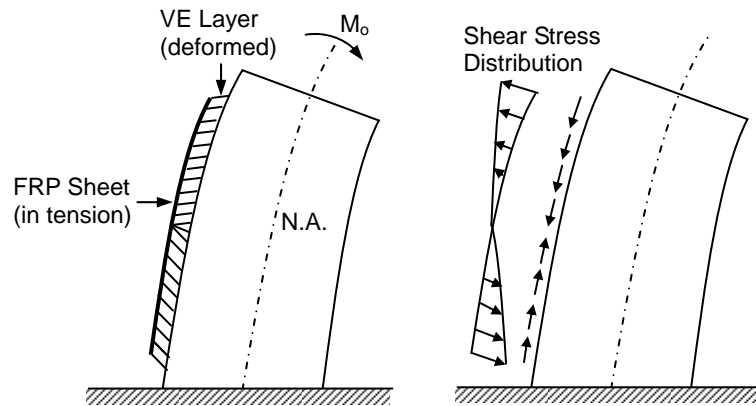


Figure 1. Shear Stress Distribution in a Conventional Layer Treatment

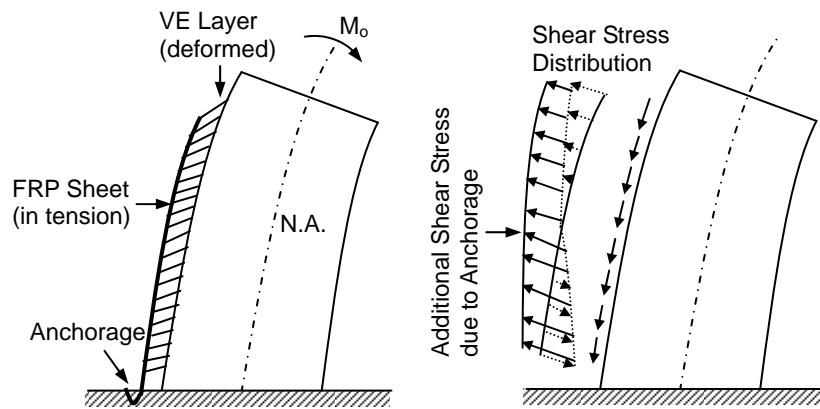


Figure 2. Shear Stress Distribution in the Proposed Layer Treatment

2.2. Equation of Motion of a Circular Column

For simplicity, the neutral axis of a circular section is assumed to pass through its center of gravity. According to the Euler beam theory, the longitudinal deformation at any point of the cross section is proportional to the distance from the neutral axis. As a result, the shear strain in the VE layer at x distance from the column footing is equal to the longitudinal deformation divided by the thickness of the VE layer. The equation of motion can thus be derived following the same procedure as used in Chen *et al.* (2006) and written as

$$EI \frac{\partial^4 y(x,t)}{\partial x^4} + m \frac{\partial^2 y(x,t)}{\partial t^2} + c \frac{\partial y(x,t)}{\partial t} + \frac{\partial \tau_{\max}(x,t)}{\partial x} \frac{\pi d^2}{8} = -m \ddot{y}_0(t) \quad (1)$$

in which EI is the flexural rigidity of the RC column, m and c are the mass and damping coefficients per unit length, respectively, which are both considered constants in this paper, $y(x,t)$ is the relative transverse

displacement with respect to the column base along the centerline of the column, $\tau_{\max}(x, t)$ is the maximum shear stress on the cross section x distance from the footing, d is the diameter of the column, and $\ddot{y}_0(t)$ is the ground acceleration.

When the base excitation $\ddot{y}_0(t) = A e^{i\omega t}$, the steady-state transverse displacement, the maximum shear stress in the VE layer can respectively be expressed as

$$y(x, t) = \phi(x) e^{i\omega t}, \text{ and } \tau_{\max}(x, t) = \frac{d}{2t_v} \frac{d\phi(x)}{dx} \frac{G'(\omega)}{\cos \delta} e^{i(\omega t + \delta)} \quad (2)$$

Here, A is the amplitude of the base acceleration, ω is the excitation frequency, t denotes the time instance, $i = \sqrt{-1}$ represents the imaginary unit of a complex number, $\phi(x)$ is a displacement function, t_v is the thickness of the VE layer, G'_v is the shear storage modulus, and δ is the loss factor of the VE material. In this study, they are taken from the experimental study by Huang (2005).

2.3. Spring Representation of the VE Layer

The 4th term on the left side of Eq. (1) represents the effect of the added VE layer. To facilitate the finite element analysis of a bridge structure, it is desirable to convert that term as a function of the transverse displacement so that it can be modeled by discrete springs of complex coefficients. A closer examination on the fourth term in Eq. (1) and the maximum stress expression in Eq. (2) indicates that the shear stress at any point is proportional to the curvature at that point for the steady-state responses. Therefore, a relation between the curvature and the displacement needs to be established. In this study, an approximation of the ratio between the curvature and the displacement of the column, $r_1(x)$, is made by using the first mode shape of the cantilever column of consistent mass (Chopra, 2001). That is,

$$r_1(x) = \beta_1^2 \frac{\cosh \beta_1 x + \cos \beta_1 x - a (\sinh \beta_1 x + \sin \beta_1 x)}{\cosh \beta_1 x - \cos \beta_1 x - a (\sinh \beta_1 x - \sin \beta_1 x)}, \quad a = \frac{\cosh \beta_1 L + \cos \beta_1 L}{\sinh \beta_1 L + \sin \beta_1 L} \quad (3)$$

where $\beta_1 = 1.8751/L$ is related to the fundamental frequency of a column of uniformly distributed mass, and L is the total length of the cantilever column. With this approximation, the 4th term on the left side of Eq. (1) can be simplified in the steady-state of vibration into the following:

$$\frac{\partial \tau_{\max}(x, t)}{\partial x} \frac{\pi d^2}{8} = \frac{\pi d^3}{16 t_v} \frac{d^2 \phi(x)}{dx^2} \frac{G'(\omega)}{\cos \delta} e^{i(\omega t + \delta)} \approx \frac{\pi d^3}{16 t_v} \frac{G'(\omega)}{\cos \delta} e^{i\delta} r_1(x) y(x, t) \quad (4)$$

The effect of the VE layer now can be approximately modeled by continuous springs along the portion of the column that is covered by the VE layer. The complex spring constant per linear length, $k(x)$, is defined as

$$k(x) = \frac{\pi d^3}{16 t_v} \frac{G'(\omega)}{\cos \delta} e^{i\delta} r_1(x) \quad (5)$$

In the FEM of a bridge structure, the effect of the VE layer can be further simplified by discrete springs. When a column is equally divided into many finite elements of Δx in length, the spring constant of the discrete element at x distance from the footing is equal to $k(x)\Delta x$ in force per length. Both the exact and approximate values of the normalized shape function $\phi(x)/\phi(L)$ are presented as a function of the normalized height x/L in Figure 4. Their corresponding exact and approximate values of the curvature-to-displacement ratio $r_1(x)/r_1(L)$ are also shown in Figure 4. It can be clearly seen from Figure 4 that both approximations are quite satisfactory. Therefore, the first

mode shape of a uniform cantilever column can be used to represent the function $r_l(x)$ in the FEM analysis of columns in a bridge structure.

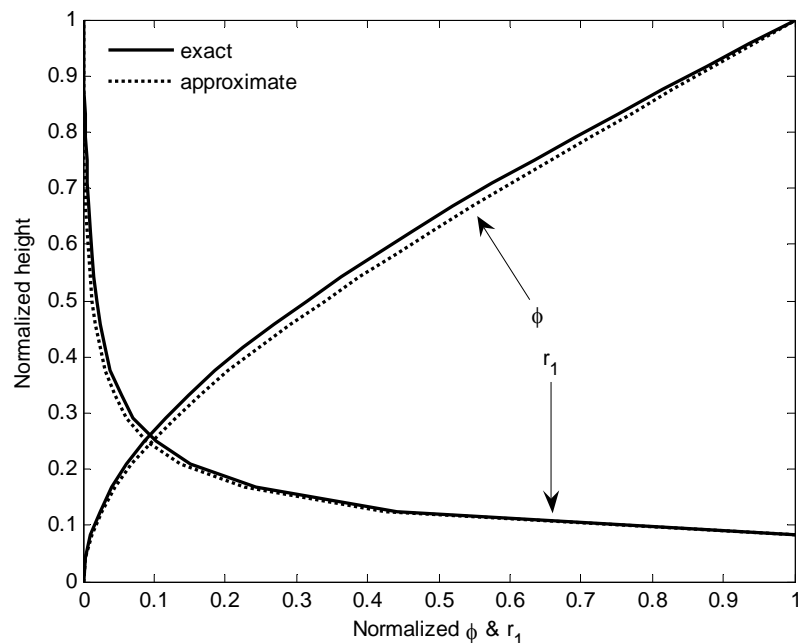


Figure 4. Normalized Shape Functions (ϕ) and Curvature to Displacement Ratios (r_1)

3. SEISMIC RETROFIT OF A HIGHWAY BRIDGE

The proposed DES methodology is applied to the seismic retrofit of the Old St. Francis River Bridge with two performance objectives. First, the bridge must be operational (Operation Performance or OP) following a moderate earthquake. Second, the bridge will not collapse during and following a strong earthquake (Collapse Prevention or CP). These performance objectives correspond to the earthquake hazards at 2% and 10% probability of exceedance in 50 years, respectively.

3.1. Old St. Francis Bridge over US60 in the New Madrid Seismic Zone

The Old St. Francis Bridge was considered as an example in this study. Designed in 1977 without seismic considerations, this 7.47 m bridge with a 20° skew angle consisted of three spans supported by steel plate girders (Chen *et. al.*, 2002). The bridge superstructure is supported by two intermediate three-column bents through one fixed bearing and one expansion bearing, along with two seat-type abutments at its ends. Both bents and abutments are supported by deep friction piles. The bridge had two expansion joints at its ends. It was built with 27.58 MPa concrete in the superstructure and 20.68 MPa concrete in the substructure as well as 275.8 MPa reinforcing steel.

The FEM of the bridge was established in SAP2000. All of the main structural components were included in the bridge model. Springs and dashpots were used at the base of each column and each abutment to model the soil and foundation effects. The periods for the first two vibration modes of the bridge were found to be 1.317s (longitudinal) and 0.477s (transverse), respectively, as shown in Figure 5.

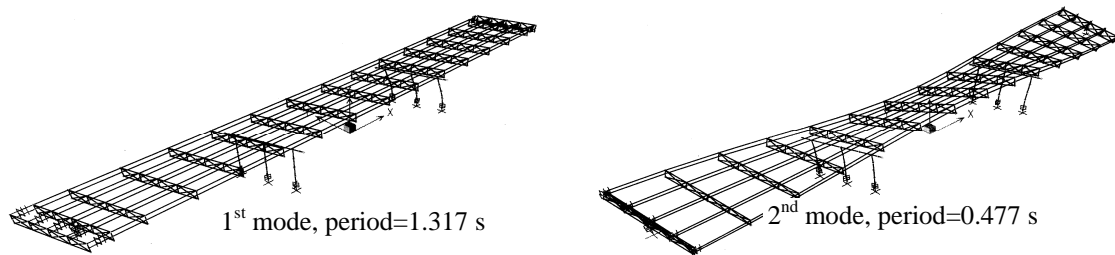


Figure 5. Vibration Periods and Mode Shapes of the Highway Bridge

3.2. Capacity/demand Ratio Evaluation of the Bridge

The capacity over demand ratio method was used to evaluate the structural condition of the bridge (FHWA, 1995; Chen *et al.*, 2002). The bridge structures have the following deficiencies:

At the operational performance (OP) level,

- Bearing failure in shear and insufficient anchorage
- Poor detailing at top and bottom of columns
- Moderate buckling of diaphragm/cross frame

At the safety performance (CP) level,

- Bearing failure in shear and insufficient anchorage
- Poor detailing at top and bottom of columns
- Column shear failure
- Significant buckling of diaphragm/cross frame

3.3. Seismic Retrofit Design Procedure

The seismic retrofit of highway bridges using the proposed methodology can be performed with the following design procedure:

- Establish multiple performance objectives such as operational and safety performance
- Strengthen the inadequate columns for shear strength and confinement at their ends with FRP sheets to meet the safety performance requirements
- Reduce the earthquake-induced forces with VE supplemental damping to meet the operational performance requirements
- Evaluate the performances of the bridge retrofitted with the damping and strengthening components.

The RC columns of the bridge were strengthened with FRP sheets of various numbers (3 or 4) of plies and/or one VE layer. The concrete and steel reinforcement properties of the columns were taken from as-built drawings (Chen *et al.*, 2002), and the FRP parameters were taken from Silva *et al.* (2007). The capacity-spectra with and without FRP wrapping (in the case of 3 plies) as well as three response spectra (demand spectra) are presented in Figure 6 according to the procedure in Fajfar (1999). The design response spectrum at the bridge site (7% probability of exceedance in 75 years) was taken from Imbsen (2007). Both moderate and strong earthquake (EQ) spectra were obtained by modifying the design spectrum to match the peak ground accelerations at 10% and 2% probability of exceedance in 50 years based on the site specific analysis by Anderson *et al.* (2001).

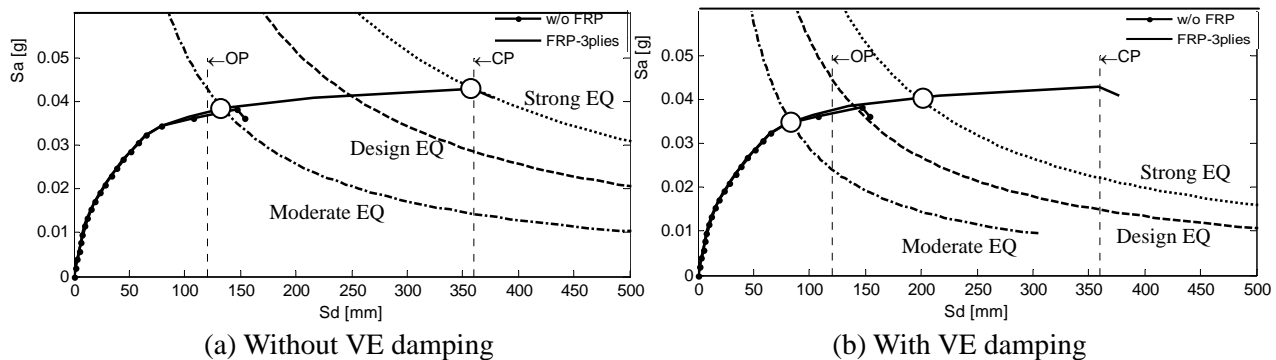


Figure 6. Capacity-demand Spectra

3.4. Results and Analysis

In Figure 6, both performance criteria are represented by specified displacements (S_d) in vertical dashed lines. The columns prior to retrofitting, Figure 6(a), satisfy neither OP nor CP. FRP strengthening alone with three plies, Figure 6(a), and VE damping alone, Figure 6(b), can satisfy the CP and OP, respectively. Only the combined use of three plies of FRP sheets and the VE damping, Figure 6(b), meet both performance objectives.

For all design options, the results of individual damping and strengthening or their combined effects are summarized in Table 1. In the table, normalized performance is defined as the ratio between the performance point (deformation) of the retrofitted column and the target performance (deformation represented by vertical dashed lines in Figure 6 both for OP and CP). The target OP and CP correspond to the ductility of 2 and 6, respectively (Priestley *et al.*, 1996). If the normalized performance or the ratio falls below 1.0, the specific design meets the intended performance objective. Note that this study is mainly focused on OP under moderate earthquakes and CP under strong earthquakes.

TABLE 1. Normalized Performance of Various Retrofit Strategies

Condition		EQ	Performance Point (mm)	Normalized Performance	
				OP	CP
w/o FRP	w/o VE Layer	Moderate	137	1.139	-
		Strong	Does not exist	-	Collapse
	w VE Layer	Moderate	84	0.698	-
		Strong	Does not exist	-	Collapse
w/o VE Layer	3 Plies FRP	Moderate	134	1.114	-
		Strong	361	-	1.003
	4 Plies FRP	Moderate	134	1.114	-
		Strong	357	-	0.993
w VE Layer	3 Plies FRP	Moderate	83	0.694	-
		Strong	198	-	0.549
	4 Plies FRP	Moderate	83	0.689	-
		Strong	197	-	0.546

It can be observed from Table 1 that, on one hand, supplemental damping alone can only reduce the bridge response and ensure that the column meet the OP requirements. In this case, the column will potentially collapse under strong earthquakes. On the other hand, strengthening with four plies of FRP sheets can meet the CP requirements; it will never meet the OP requirements. The combined use of three plies of FRP sheets and one VE layer will meet both the OP and CP requirements. Furthermore, the normalized performance (0.694 and 0.549) are not so far apart, indicating some level of consistency in terms of the margin of compliance. The optimal solution may be achievable after various percentages of VE coverage on columns have been investigated.

4. CONCLUDING REMARKS

The end goal of the proposed new methodology is to enable engineers to retrofit a bridge structure for its normalized performances against multiple objectives under different levels of earthquake hazards. This paper presents one significant step towards that goal, developing a finite element modeling technique for the implementation of this methodology in practical applications. Specifically, discrete springs were introduced to model the effects of distributed VE damping layers on the response of columns and the structural system at large. The discrete spring model was validated against the analytical solution and found quite satisfactory.

The validated model was then applied to the seismic retrofit of the Old St. Francis River Bridge in the New Madrid Seismic Zone. The normalized performance of columns is investigated with the proposed DES methodology for multiple performance objectives. It was observed that damping satisfies the operational performance under moderate earthquakes, and strengthening only ensures the safety performance under strong earthquakes. Only the combined efforts of both damping and strengthening can meet multiple performance objectives under earthquakes of various intensities.

5. ACKNOWLEDGEMENTS

Financial support to complete this study was provided in part by the Center for Transportation Infrastructure and Safety (CTIS), a national University Transportation Center at the Missouri University of Science and Technology through its Graduate Student Fellowship Program and by Ameren, St. Louis, MO, through a research contract on the seismic vulnerability assessment of power substations. These supports are greatly appreciated.

REFERENCES

- ATC/MCEER Joint Venture (2001). Recommended LRFD Guidelines for the Seismic Design of Highway Bridges, Applied Technology Council.
- Chen, G., Wang, W., and Huang, X. (2006). Optimal design of RC column seismic retrofitting for multiple performance objectives with an integrated damping and strengthening methodology. Presented at the 8th National Conference on Earthquake Engineering (CD-Rom), San Francisco, April 17-21.
- Chen, G., Thebeau, P., and Mu, H. (2002). Seismic vulnerability of highway bridges along a designated emergency vehicle access routes near the New Madrid Seismic Zone. Presented at the 7th National Conference on Earthquake Engineering (CD-Rom), Boston, July 21-25.
- Chopra, A. K. (2001). Dynamics of Structures. Prentice Hall, New York.
- Fajfar, P. (1999). Capacity spectrum method based on inelastic demand spectra. *Earthquake Engineering and Structural Dynamics* **28**, 979-993.
- FEMA-273 (1997). NEHRP Guidelines for the Seismic Rehabilitation of Buildings, Building Seismic Safety Council, 1997.
- FHWA (1995). Seismic Retrofitting Manual for Highway Bridges, Federal Highway Administration, Publication No. FHWA-RD-94-052.
- Huang, X. (2005). An Integrated VE Damping and FRP Strengthening System for Performance-based Seismic Retrofit of RC Columns. *Ph.D. Dissertation* submitted to the Graduate Faculty of the University of Missouri-Rolla, 2005.
- Imbsen, R. A. (2007). AASHTO Guide Specifications for LRFD Seismic Bridge Design. *A Draft Proposal to Subcommittee for Seismic Effects on Bridges T-3*.
- Kerwin, E. M. and Ungar, E. E. (1990). Requirements imposed on polymeric materials by structural damping applications. *Sound and Vibration Damping with Polymers* (Ed. Corsaro RD and Sperling LH). ACS Series 424, 317-345.
- MCEER (2005). Seismic Retrofitting Manual for Highway Structures: Part 1 – Bridges, Working Draft,



- Prepared by the Multidisciplinary Center for Earthquake Engineering Research (MCEER) for Federal Highway Administration.
- Priestley, M.J.N, Seible, F., and Calvi, G.M. (1996). *Seismic Design and Retrofit of Bridges*, John Wiley & Sons, New York.
- Silva, P.F., Erecson, N.J., and Chen, G.D. (2007). Seismic retrofit of bridge joints in Central U.S. with carbon fiber-reinforced polymer composites. *ACI Structures Journal* **104:2**, 207-217.
- Soong, T.T. and Dargush, G.F. (1997). *Passive Energy Dissipation System in Structural Engineering*, John Wiley & Sons, New York.